

PHYSICS OF MAGNETIC PHENOMENA

MAGNETIC PROPERTIES OF THE $\text{Hg}_{1-x}\text{Mn}_x\text{S}$ CRYSTALS

P. D. Mar'anchuk and G. O. Andrushchak

UDC 621.315.592

The magnetic susceptibility χ of $\text{Hg}_{1-x}\text{Mn}_x\text{S}$ is investigated at temperatures $T = 77\text{--}300\text{ K}$ for $H = 4\text{ kOe}$ by the Faraday method before and after thermal treatment of the sample in compound vapors. The special features of χ are found to be caused by the presence in the crystals of Mn–S–Mn–S clusters of different sizes in which indirect antiferromagnetic exchange interaction of the Mn atoms occurs through the chalcogen atoms. Thermal treatment of samples in compound vapors causes changes of sizes of clusters existing in the crystal and even dissipation of the second-phase inclusions.

INTRODUCTION

The $\text{Hg}_{1-x}\text{Mn}_x\text{S}$ solid solutions are semiconductors whose gap width (E_g) changes depending on the structure; they belong to semimagnetic semiconductors. The Mn atoms with uncompensated magnetic moments presented in the samples enable the researchers to control the structure (x) and presence of the second-phase inclusions in the samples by the magnetic methods (in particular, by measuring the magnetic susceptibility of crystals).

The $\text{Hg}_{1-x}\text{Mn}_x\text{S}$ semimagnetic semiconductor solid solutions (that exist for $0 < x \leq 0.375$) [1] obtained by us by the Bridgeman method had the n -type intrinsic conductivity (with electron concentration $n \sim 10^{18}\text{ cm}^{-3}$).

RESULTS OF INVESTIGATIONS AND THEIR DISCUSSION

The magnetic susceptibility χ of the $\text{Hg}_{1-x}\text{Mn}_x\text{S}$ samples was investigated by the Faraday method at temperatures $T = 77\text{--}300\text{ K}$ and $H = 4\text{ kOe}$. Figure 1 shows the temperature dependence of the magnetic susceptibility of $\text{Hg}_{1-x}\text{Mn}_x\text{S}$ samples. From the figure it can be seen that the shape of the dependences $\chi = f(T)$ is characteristic of paramagnetics, namely, the magnetic susceptibility increases with decreasing temperature (due to a decreased misorienting effect of thermal oscillations of crystal lattice atoms on the orientations of magnetic moments of the Mn atoms in the magnetic field direction). A peak is seen in the dependence $\chi = f(T)$ (curve 2) with a maximum at $T \sim 200\text{ K}$ (typical of the antiferromagnets). This peak can be caused by the presence of the second-phase inclusions in the $\text{Hg}_{1-x}\text{Mn}_x\text{S}$ crystal, to be exact, by their transition from the magnetically ordered to paramagnetic state at the Néel temperature ($T = T_N$). The presence of the second-phase inclusion in the sample with $x_M = 0.027$ can be confirmed by the fact that its magnetic susceptibility at low temperatures is less than χ of the sample with $x_M = 0.017$. This is explained by antiferromagnetic magnetic ordering that arises in the second-phase inclusions at low temperatures; as a result, the magnetic moments of Mn atoms (which are incorporated into the second phase) are mutually compensated and do not contribute to χ (therefore, χ for $x_M = 0.027$ is less than for $x_M = 0.017$ in which the magnetic ordering and exchange interaction are absent: $\theta = 0$).

The magnetic susceptibility of manganese atoms is determined from the formula

Chernovtsy National University, Chernovtsy, Ukraine, e-mail: p.maryanchuk@chnu.edu.ua. Translated from Izvestiya Vysshikh Uchebnykh Zavedenii, Fizika, No. 3, pp. 59–63, March, 2008. Original article submitted July 30, 2007.

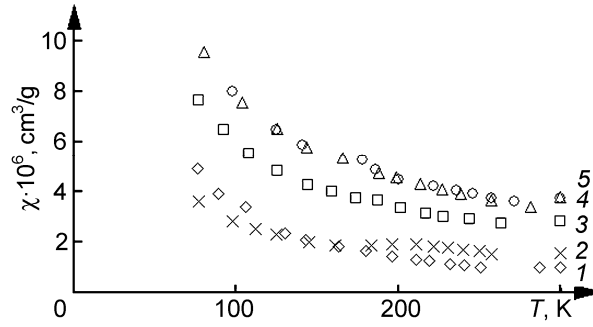


Fig. 1. Temperature dependence of the $\text{Hg}_{1-x}\text{Mn}_x\text{S}$ magnetic susceptibility for $x_M=0.017$ (curve 1), 0.027 (curve 2), 0.042 (curve 3), 0.059 (curve 4), and 0.069 (curve 5).

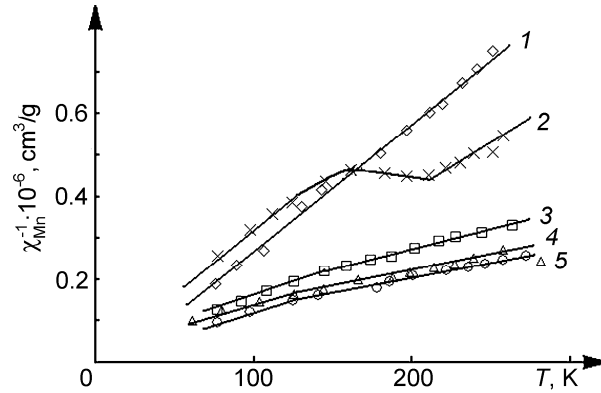


Fig. 2. Temperature dependence of χ_{Mn}^{-1} for $\text{Hg}_{1-x}\text{Mn}_x\text{S}$ with $x_M=0.017$ (curve 1), 0.027 (curve 2), 0.042 (curve 3), 0.059 (curve 4), and 0.069 (curve 5).

$$\chi_{\text{Mn}} = \chi - \chi_{\text{HgS}}, \quad (1)$$

where χ is the measured $\text{Hg}_{1-x}\text{Mn}_x\text{S}$ magnetic susceptibility and χ_{HgS} is the HgS magnetic susceptibility.

It can be seen from Fig. 2 that the dependences $\chi_{\text{Mn}}^{-1} = f(T)$ are linear (with different slopes) and are described by the Curie or Curie–Weiss law:

$$\chi = \frac{C}{T - \theta}, \quad (2)$$

where C is the Curie constant:

$$C = \frac{xN_0g^2S(S+1)\mu_B^2}{3k_B M_0}. \quad (3)$$

Here N_0 is the Avogadro number, $M_0 = \Gamma\text{M}$ is the molecular weight of $\text{Hg}_{1-x}\text{Mn}_x\text{S}$, x specifies the Mn content, and μ_B is the Bohr magneton.

The negative paramagnetic Curie temperatures ($\theta < 0$) indicate that the antiferromagnetic exchange interaction of the Mn atoms occurs in $\text{Hg}_{1-x}\text{Mn}_x\text{S}$ crystals ($x_M=0.017$). We now consider possible types of the second-phase

TABLE 1. Magnetic Parameters of the $\text{Hg}_{1-x}\text{Mn}_x\text{S}$ Samples

x_M	θ , K	$\mu_{\text{eff}}(\mu_B)$	T_C , K
0.017	0	5.92	–
0.042	–12	5.05	125
	–63	6.05	
0.059	–15	5.16	117
	–58	5.65	
0.069	–15	4.81	135
	–85	5.90	

TABLE 2. Magnetic Parameters of the $\text{Hg}_{1-x}\text{Mn}_x\text{S}$ Samples

x_M	n , cm^{-3} (at $T = 300$ K)		θ , K		μ_{eff} , μ_B (per Mn atom)	
	Before annealing	After annealing	Before annealing	After annealing	Before annealing	After annealing
Before and after annealing in mercury vapor						
0.027	$8.6 \cdot 10^{17}$	$1.2 \cdot 10^{18}$	–38	–15	5.72	5.63
			–6	–50	4.4	6.84
Before and after annealing in sulfur vapors						
0.017	$9.9 \cdot 10^{17}$	$5.9 \cdot 10^{17}$	0	–5	5.92	5.92
0.042	$8.7 \cdot 10^{17}$	$3.1 \cdot 10^{17}$	–12	–33	5.05	5.04
			–63	–156	6.05	6.32

inclusions and clusters (which correspond to them by the character of exchange interaction, but unlike the phases, have no intrinsic crystal structure and are formed based on the structure of the crystal in which they exist) in the $\text{Hg}_{1-x}\text{Mn}_x\text{S}$ crystals. MnS_2 ($T_N = 60$ K and $\theta = -592$ K), MnS ($T_N = 155$ K and $\theta = -982$ K), and Mn ($T_N = 100$ K) belong to the phases that could be formed in the examined crystals (the MnO phase with $T_N = 120$ K or clusters corresponding to it are less probable than these ones). All these phases are ferromagnetic, and if they are present in $\text{Hg}_{1-x}\text{Mn}_x\text{S}$, they will cause the appearance of the special features (peaks) in the temperature dependence of the magnetic susceptibility at the Néel temperatures T_N (for example, a peak (maximum) in the dependence $\chi = f(T)$ is observed for the sample with $x_M = 0.027$ at $T \sim 200^\circ\text{C}$, which testifies to the presence of the second-phase inclusions (MnS , see curve 2 in Fig. 1) in the $\text{Hg}_{1-x}\text{Mn}_x\text{S}$ sample). In clusters of these phases, the antiferromagnetic exchange interaction (antiferromagnetic ordering) can be weaker or stronger depending on the cluster sizes and temperatures. With increasing cluster sizes, the paramagnetic Curie temperature θ and the bending temperature T_C for the dependence $\chi_{\text{Mn}}^{-1} = f(T)$ increase approaching to their values for clusters of the MnS_2 , MnS , and Mn phases; in the case of precipitation of phases, these parameters will coincide.

The foregoing allows us to consider that the Mn-S-Mn-S clusters are most typical of the $\text{Hg}_{1-x}\text{Mn}_x\text{S}$ crystals, and the character of their exchange interaction is analogous to that of the MnS phase, because they are formed by isovalent substitution of the mercury atoms by the Mn atoms in the $\text{Hg}_{1-x}\text{Mn}_x\text{S}$ crystals.

Thus, bending in the dependence $\chi_{\text{Mn}}^{-1} = f(T)$ at $T = T_C$ is caused by transition of the Mn-S-Mn-S clusters of different sizes (in which indirect antiferromagnetic exchange interaction of the Mn atoms occurs through the sulfur atoms by analogy with $\text{Hg}_{1-x}\text{Mn}_x\text{Se}$ [2, 3]) to the paramagnetic state with increasing temperature. Moreover, the cluster transition from the antiferromagnetic to paramagnetic state is almost invisible in the dependence $\chi = f(T)$ (see fig. 1). The increase in the effective magnetic moment of the Mn atoms (μ_{eff}) with temperature (see Table 1) confirms that the clusters pass from the antiferromagnetic to paramagnetic state at $T = T_C$.

The parameters calculated from the dependence $\chi_{\text{Mn}}^{-1} = f(T)$ measured for the $\text{Hg}_{1-x}\text{Mn}_x\text{S}$ samples, namely, the content of the magnetic compound x_M (retrieved from the average high-temperature sections of the dependence

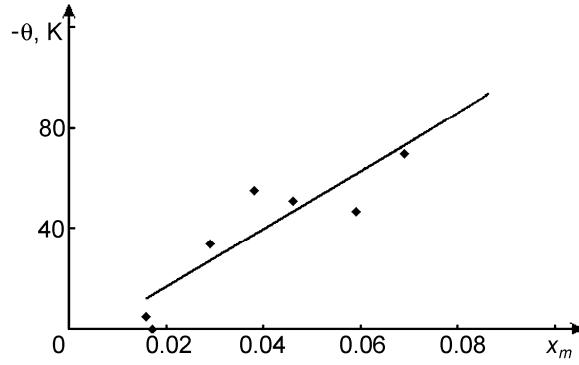


Fig. 3. Dependence of the paramagnetic Curie temperature on the $\text{Hg}_{1-x}\text{Mn}_x\text{S}$ sample structure.

$\chi_{\text{Mn}}^{-1} = f(T)$ at $T = 300 \text{ K}$), paramagnetic Curie temperature θ , bending temperature T_C , and the effective magnetic moment of manganese atoms μ_{eff} are tabulated in Tables 1 and 2. For the given x_M , the lower row of the parameters is presented for a higher-temperature section of the dependence $\chi_{\text{Mn}}^{-1} = f(T)$. Extrapolation of the dependences $\chi_{\text{Mn}}^{-1} = f(T)$ averaged over high temperatures and described by Curie–Weiss law yields θ values for samples with structure x_M retrieved from the dependences $\chi_{\text{Mn}}^{-1} = f(T)$ and formulas (2) and (3).

In the high-temperature approximation $k_B T \gg \epsilon_A$, where ϵ_A is the energy of exchange interaction of the atoms with intrinsic magnetic moments, Spalek *et al.* [4] obtained the following expression for the paramagnetic Curie temperature:

$$\theta(x) = -\frac{2}{3} x S(S+1) \sum_p J_p \frac{Z_p}{k_B} = \theta_0 x, \quad (4)$$

where J_p is the integral of exchange interaction of neighboring pairs and Z_p is the number of cation states in the p -coordination sphere. The constant θ_0 is the limiting value of $\theta(x)$ for the hypothetical magnetic semiconductor with $x = 1$ and $A^{II}B^{\text{VI}}$ semiconductor structure.

Expression (4) allows the exchange integral J_1 to be estimated for neighboring pairs in the first coordination sphere ($Z = 12$):

$$2 \cdot \frac{J_1}{k_B} = 3 \frac{\theta_0}{Z \cdot S \cdot (S+1)}. \quad (5)$$

The experimental dependence $\theta(x)$ for $\text{Hg}_{1-x}\text{Mn}_x\text{S}$ is described by a straight line (Fig. 3). Extrapolation of this dependence toward $x = 1$ gives $\theta_0 = -990 \text{ K}$. This θ_0 value determines the exchange integral for Mn–S–Mn pairs ($J_1/k_B = -14.1 \text{ K}$).

During thermal treatment of the $\text{Hg}_{1-x}\text{Mn}_x\text{S}$ crystals which possess clearly pronounced subsystems of defects and clusters, the possibilities arise for diffusion of compound vapor atoms into the crystal (during annealing), escape of atoms from lattice sites, their migration through the crystal, and occupation of different places in the crystal lattice, including vacancies, interstices, and sites.

The system of defects in this case can facilitate the decrease or increase of the clusters sizes and formation of new clusters, which is manifested through changes of the kinetic crystal parameters (the defects are electrically active) and magnetic parameters (the paramagnetic Curie temperature θ and the effective magnetic moment of manganese atoms μ_{eff} , see Table 2) of the samples and hence the dependences $\chi_{\text{Mn}}^{-1} = f(T)$ from which they are calculated (see Fig. 4).

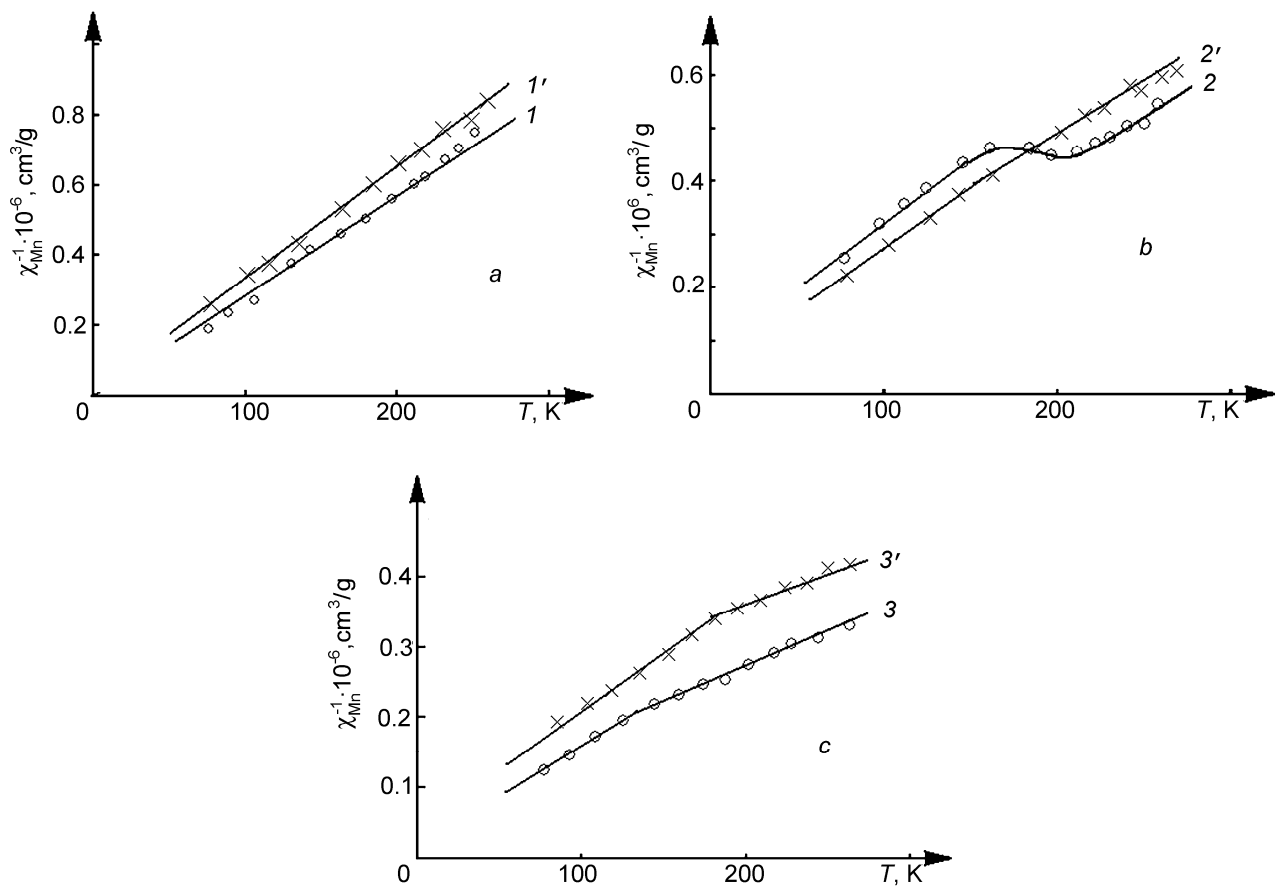


Fig. 4. Temperature dependence of χ_{Mn}^{-1} for $\text{Hg}_{1-x}\text{Mn}_x\text{S}$: a) $x_M = 0.017$ before (curve 1) and after annealing in sulfur vapors (curve 1'); b) $x_M = 0.027$ before (curve 2) and after annealing in mercury vapors (curve 2'); c) $x_M = 0.042$ before (curve 3) and after annealing in sulfur vapors (curve 3').

Thus, thermal treatment of the $\text{Hg}_{1-x}\text{Mn}_x\text{S}$ samples in compound vapor, by analogy with $\text{Hg}_{1-x}\text{Mn}_x\text{Se}$ [5], leads to changes of sizes of clusters already existing in the crystals (the cluster sizes are proportional to θ) and even to dissipation of the second-phase inclusions (that is, to a decrease in their sizes and transformation of the second MnS phase inclusions into the Mn–S–Mn–S clusters).

CONCLUSIONS

1. The peaks of the dependences $\chi = f(T)$ at $T = T_N$ and sharp (stepwise) changes of χ at $T = T_N$ in the dependences $\chi_{\text{Mn}}^{-1} = f(T)$ testify to the presence of the second-phase inclusions in the $\text{Hg}_{1-x}\text{Mn}_x\text{S}$ crystals.

2. The presence in the $\text{Hg}_{1-x}\text{Mn}_x\text{S}$ crystals of Mn–S–Mn–S clusters of different sizes in which the indirect antiferromagnetic exchange interaction of the Mn atoms occurs through the sulfur atoms and their transition from the antiferromagnetic into the paramagnetic state with increasing temperature are manifested in the dependences $\chi_{\text{Mn}}^{-1} = f(T)$ which bend at $T = T_C$ and change the slopes of their rectilinear sections.

3. The increase of the effective magnetic moment of Mn atoms μ_{eff} (determined by the slope of the rectilinear section of the dependence $\chi_{\text{Mn}}^{-1} = f(T)$) with temperature confirms that at $T = T_C$, the clusters pass from the antiferromagnetic to the paramagnetic state.

4. Thermal treatment of samples in compound vapors causes the sizes of clusters existing in the crystal to change and the second-phase inclusions to dissipate (that is, their sizes decrease and the second MnS phase inclusions are transformed into the Mn–S–Mn–S clusters).

REFERENCES

1. V. N. Tomashik and V. I. Grytsiv, Phase Diagrams of Systems Based on $A^{II}B^{VI}$ Semiconductor Compounds [in Russian], Naukova Dumka, Kiev (1982).
2. P. D. Mar'anchuk, *Izv. Vyssh. Uchebn. Zaved., Fiz.*, No. 1, 122–124 (1984).
3. P. D. Mar'anchuk and N. P. Gavaleshko, *Izv. Akad. Nauk SSSR, Neorg. Mater.*, **23**, No. 8, 1271–1274 (1987).
4. J. Spalek, F. Lewicki, Z. Tarnawski, *et al.*, *Phys. Rev.*, **B33**, No. 5, 3407 (1986).
5. P. D. Mar'anchuk, *Russ. Phys. J.*, No. 8, 753–757 (1993).